ARTICLE

Photocatalysis with CdSe Nanoparticles in Confined Media: Mapping Charge Transfer Events in the Subpicosecond to Second Timescales

Clifton Harris and Prashant V. Kamat*

Radiation Laboratory and Department of Chemistry and Biochemistry, University of Notre Dame, Notre Dame, Indiana 46556

ABSTRACT Photoinduced charge transfer events between 3 nm diameter CdSe semiconductor nanocrystals and an electron acceptor, MV^{2+}, have been probed in the subpicosecond—microseconds—seconds time scale by confining the reactants in an AOT/heptane reverse micelle. The probe molecule, methyl viologen (MV^{2+}) interacts with the excited CdSe nanoparticle and quenches its emission effectively. The ultrafast electron transfer to MV^{2+}, as monitored from the exciton bleaching recovery of CdSe and the formation of $MV^{+\bullet}$ radical, is completed with an average rate constant of 2.25×10^{10} s^{-1}. Under steady state irradiation (450 nm) the accumulation of $MV^{+\bullet}$ is seen with a net quantum yield of 0.1. Mediation of the electron transfer through TiO_2 nanoparticles is achieved by coupling them with the CdSe-MV^{2+} system within the reverse micelle. This coupling of two semiconductor nanoparticles increases the quantum yield of MV^{2+} reduction by a factor of 2. The dual roles of TiO_2 as an electron shuttle and a rectifier are elucidated by transient absorption spectroscopy and steady state photolysis. The presence of both TiO_2 and MV^{2+} in the reverse micelle creates a synergistic effect to enhance the electron transfer rate constant by an order of magnitude. The time-resolved events that dictate the production and stabilization of electron transfer product provide an insight into the photocatalytic systems that are potentially important in solar hydrogen production and photocatalytic remediation.

KEYWORDS: light energy conversion · artificial photosynthesis · photoinduced electron transfer · semiconductor nanocrystals · photocatalysis · reverse micelles · CdSe · viologen radical

Interfacial electron transfer in semiconductor nanoparticles systems has drawn significant interest because of its application to solar cells,[1,2] photocatalysis,[3−6] environmental remediation,[7,8] and solar hydrogen production.[3] Bandgap excitation of the semiconductor nanoparticles results in charge separation. Because of the small size (a few nanometers in diameter), the majority of these charge carriers recombine *via* nonradiative or radiative processes. Only a small fraction (<10%) of these photogenerated electrons and holes can be utilized to initiate the redox processes at the interface. Coupling two semiconductors (*e.g.*, CdS/TiO_2,[9−12] CdSe/ZnO,[13−15] TiO_2/SnO_2[16,17]) with suitable energetics can significantly improve the selectivity and enhance the charge separation yield. The interfacial charge transfer events investigated by different techniques on different time scales draw varying conclusions depending upon the event and time scale being probed. Controversies often emerge regarding the quantum efficiency and the rate of charge transfer.[18] The present study is aimed at providing a better understanding of the events that influence the photoconversion yields and mapping out the charge transfer kinetics at different timescales.

Reverse micelles are thermodynamically stable nanostructures composed of a polar core encapsulated by surfactant molecules in nonpolar media. These structures enable the synthesis of semiconductor nanoparticles.[19] In previous studies reverse micelles have been used to synthesize size-controlled CdS[20−23] and CdSe[24] nanocrystals in heptane/water/AOT. The surfactant, dioctyl sulfosuccinate, commonly known as Aerosol-OT (AOT) is the preferred choice for attaining reverse micelles in nonpolar media because of its ability to accommodate spherical water pools of controlled sizes.[25] The size of the water pool, which is dependent on the molar water-to-surfactant ratio, $w_o = [H_2O]/[AOT]$,[26] directly controls the size of the semiconductor particle synthesized within the confined polar volume.[22,24] Additionally, one can vary other parameters such as the ratios of precursor concentrations, temperature, and pH to control the particle size of CdSe nanoparticles.[27,28]

Because of their size dependent absorption and emission properties CdSe nanoparticles have been the choice of many recent electron transfer investigations.[29−37] Reverse micelles provide a quick, low cost, room temperature methodology to synthe-

*Address correspondence to pkamat@nd.edu.

Received for review December 10, 2008 and accepted February 04, 2009.

Published online February 18, 2009.
10.1021/nn800848y CCC: $40.75

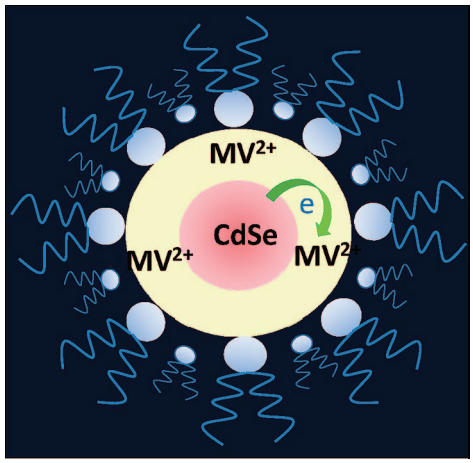

Scheme 1. Electron transfer between CdSe and methyl viologen in a confined medium.

size quantized CdSe nanoparticles of a narrow size distribution.[24] Reverse micelles also allow for control of the medium immediately surrounding the CdSe nanoparticles as well as the incorporation of electron acceptor molecules. Scheme 1 shows a schematic diagram of the semiconductor and methyl viologen assembly within the polar core of the reverse micelle. Electrons accumulated within the conduction band of the CdSe (E_{CB} = −0.6 V *vs* NHE)[38] are energetic enough to transfer to MV^{2+} (E^0 ($MV^{2+}/MV^{+\bullet}$) = −0.445 V *vs* NHE)[39] and TiO_2 (E_{CB} = −0.5 V *vs* NHE).[33,39] The electron transfer between CdSe−MV^{2+} and CdSe−TiO_2 has been probed by several research groups.[30,32,33,40−43] Because of its pH independent redox properties viologen compounds have been used as a probe to investigate electron transfer reactions in semiconductor particulate systems.[44] An in-depth analysis of the charge transfer events at different timescales (subpicosecond to minutes), however, is lacking.

The efficiency and kinetics of interparticle electron transfer between CdSe and MV^{2+} and the stabilization of electron transfer product ($MV^{+\bullet}$) have now been investigated using time-resolved transient spectroscopy in different time domains. In addition, the effect of TiO_2 as an electron mediator for enhancing the electron transfer yield has also been investigated. A better understanding of the electron transfer processes in a confined medium should enable one to develop efficient solar energy harvesting assemblies.

RESULTS AND DISCUSSION

Absorption and Emission Characteristics. CdSe nanoparticles synthesized in reverse micelle suspensions show size quantization effects. The size of the water pool radius, which provides the control of the CdSe particle diameter, is proportional to w_o for $1 \geq w_o \geq 20$. In the present experiments we maintained w_0 = 9.4 in order to obtain a water pool of diameter ~8 nm. Figure 1 shows the absorption and emission spectra of CdSe and the absorption spectrum of TiO_2 nanoparticles em-

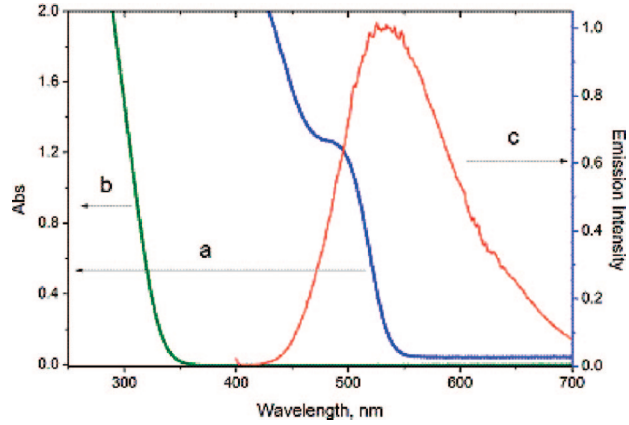

Figure 1. Absorption spectra of (a) 6.6 μM CdSe and (b) 20 μM TiO_2 nanoparticles in AOT/heptane; (c) the emission spectrum of CdSe nanoparticles. Normalized to 1.

ployed in the present study. The CdSe nanoparticles exhibit a characteristic exciton band at 500 nm and emission maximum at 540 nm. Based on the excitonic peak position (500 nm) we estimate the diameter of the CdSe particle to be ~3 nm and thus confirm it to be in the quantized regime.[45] The absorption of TiO_2 nanoparticles (<5 nm diameter) shows onset of absorption below 370 nm thus representing relatively large bandgap. We determined the particle concentration [p] of the stock solution by dividing molar concentration [C] with the agglomeration number *n* (equation 1)

$$[p] = [C] / n$$
$$\text{where } n = (4 / 3\pi N_a r^3) / V_m = 2525 r^3 / V_m \qquad (1)$$

V_m is the molar volume of the semiconductor, *r* is the particle radius in nm, and N_a is Avogadro's number. All concentrations reported are particle concentrations.

Interaction between Excited CdSe and Methyl Viologen. CdSe nanoparticles undergo charge transfer at the interface following bandgap excitation. Methyl viologen is a suitable probe for identifying the factors responsible for interfacial charge transfer in semiconductor photocatalyst systems. A micellar stock solution of 6 mM MV^{2+} (w_o

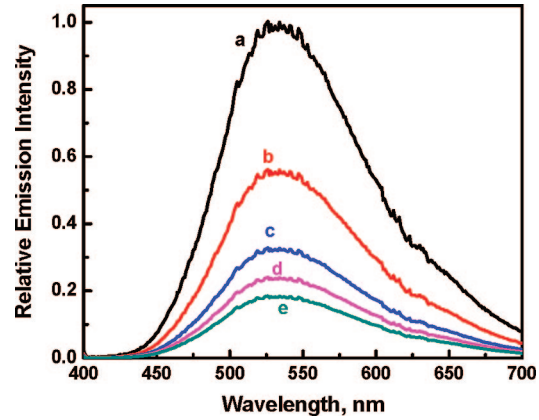

Figure 2. Emission of 6.6 μM CdSe in AOT/heptane: (a) 0, (b) 0.66, (c) 1.21, (d) 1.64, and (e) 2.00 mM MV^{2+} (excitation wavelength 400 nm).

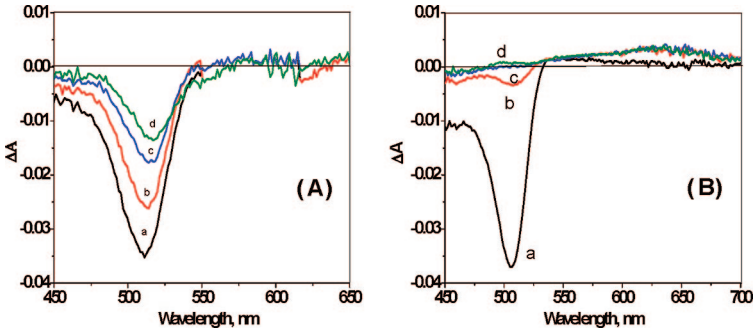

Figure 3. Transient absorption spectra recorded following 387 nm laser pulse excitation of 2.2 μM CdSe nanoparticles in AOT/heptane (A) in the absence and (B) in the presence of 2 mM MV^{2+}. The difference absorbance spectra were recorded (a) 2 ps, (b) 40 ps, (c) 400 ps, and (d) 1.2 ns after laser pulse excitation.

= 9.4) was prepared by mixing an aqueous solution of MV^{2+} with AOT/heptane under rapid stirring. A known amount of the MV^{2+} in AOT/heptane was then mixed with the CdSe suspension in AOT/heptane to probe the interaction with excited CdSe nanoparticles. Figure 2 shows CdSe emission spectra recorded at different concentrations of MV^{2+}. With increasing concentration of MV^{2+} we observed a decrease in emission. The emission quenching represents excited-state interaction between excited CdSe and MV^{2+} to induce electron transfer at the interface (reactions 2−5),

$$\mathrm{CdSe} + h\nu \rightarrow \mathrm{CdSe(h + e)} \quad (2)$$

$$\mathrm{CdSe(h + e)} \rightarrow \mathrm{CdSe} + h\nu' \quad (3)$$

$$\mathrm{CdSe\ (h + e)} + \mathrm{MV^{2+}} \rightarrow \mathrm{CdSe\ (h_t)} + \mathrm{MV^{+\bullet}} \quad (4)$$

$$\mathrm{CdSe\ (h_t)} + \mathrm{MV^{+\bullet}} \rightarrow \mathrm{CdSe} + \mathrm{MV^{2+}} \quad (5)$$

where h and e represent holes and electrons, respectively, and h_t represents shallow and deep-trap holes. The effective quenching of CdSe emission seen at such low concentrations of MV^{2+} is an indication that these molecules are associated with CdSe and represent static quenching of CdSe emission. The association constant for the interaction between the CdSe quantum dots and MV^{2+}/TiO_2 was determined from the double reciprocal plot analysis.[12,46] The linear plot of $1/(\Theta - \Theta_{obsd})$ *versus* $1/[MV^{2+}]$ gave a value of 644 ± 34 M^{-1} for a CdSe−MV^{2+} system. In a similar fashion we also analyzed the quenching of CdSe emission by TiO_2 nanoparticles. The value of the association constant for the CdSe−TiO_2 complex was 3.2 ± 0.3 × 10^5 M^{-1}. (see Figures S1 and S2 in Supporting Information for the plots and analysis.)

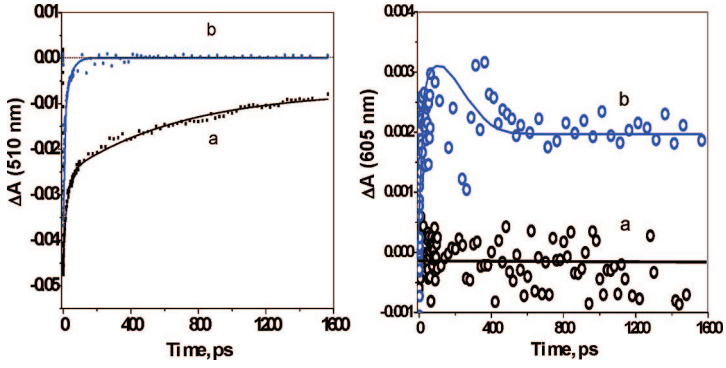

Figure 4. Absorption-time profiles monitored at (left) 510 nm and (right) 605 nm following 387 nm laser pulse excitation of 2.2 μM CdSe nanoparticles in AOT/heptane in the (a) absence and (b) presence of 2 mM MV^{2+}. The biexponential fit are shown as sold lines.

Photoinduced Electron Transfer. As shown earlier[30,33,41,42,47,48] the ultrafast charge transfer dynamics in semiconductor nanoparticle systems can be probed with femtosecond transient absorption spectroscopy. For example, El-Sayed and co-workers[47] demonstrated that the electron transfer between CdS and methyl viologen occurs within 200−300 fs to produce relatively stable viologen radicals. In a follow-up study[30] they probed the electron transfer between CdSe and quinones. The ultrafast electron transfer from excited CdSe to quinone was followed by the rapid decay of the radical ion with a decay lifetime of 2.5 ps indicating the failure to achieve long-lived charge stabilization. By comparing the stabilities of the electron transfer products the researchers were able to identify the role of acceptor molecule as electron shuttle or sink.[30]

The transient absorption spectra recorded following laser pulse excitation of CdSe nanoparticles in the absence and presence of MV^{2+} are shown in Figure 3 panels A and B, respectively. In the absence of MV^{2+} the photoinduced charge separation results in the bleaching of the CdSe excitonic band. Nearly 80% of the bleaching recovery is seen during the period of 1.6 ns as these charge carriers undergo recombination or are transferred across the semiconductor interface to an electron shuttle or sink. The charge recombination dynamics of CdSe nanocrystals has been discussed in detail.[36,37,48−52] In the presence of MV^{2+} we observed a quick recovery of the bleaching, within 100 ps, indicating fast disappearance of photogenerated electrons from CdSe nanocrystals. The simultaneous appearance of the absorption band in the red region (broad maximum at ~605 nm) confirms the interfacial electron transfer to MV^{2+} to produce $MV^{+\bullet}$ radical. The formation of $MV^{+\bullet}$ reflects an ultrafast interfacial charge transfer event and agrees with the observation made in the transient absorption study of CdS and $MV^{2+\bullet}$.[47]

The bleaching recovery of the CdSe at 510 nm (Figure 4A) was analyzed using biexponential fit (equation 6) and the results are summarized in Table 1.

$$\Delta A(t) = a_1 e^{(t/\tau_1)} + a_2 e^{(t/\tau_2)} \quad (6)$$

Parameters a_1 and a_2 are the relative amplitudes of each lifetime; τ_1 and τ_2 are the fast and slow components of the excited-state lifetime, respectively. The average lifetime, $\langle\tau\rangle$, is determined from the equation $\langle\tau\rangle$

$= [\sum(a_i\tau_i^2)]/\sum(a_i\tau_i)]$.[53] The average rate constant for the disappearance of electrons, k, is obtained from the reciprocal value of average lifetime. The bleaching recovery of CdSe alone exhibited an average lifetime of 348 ± 18 ps. In the presence of methyl viologen the average lifetime decreased to 44 ps, suggesting a rapid disappearance of electrons as they are transferred to the acceptor molecules. The electron transfer occurs with a rate constant of $2.25 \pm 0.12 \times 10^{10}$ s^{-1}. By comparing the average rate constants (Table 1) of CdSe bleaching recovery with MV^{2+} (e−h recombination + electron transfer) and without MV^{2+} (e−h recombination), we calculated that 87% of the electrons generated following the laser pulse excitation are transferred across the interface. The fast component (τ_1 = 3.26 ps) of the recovery, however, indicates an upper limit for the time constant for the electron transfer. Indeed, the growth of absorption at 605 nm confirms the production of $MV^{+\bullet}$ within a period of 10 ps.

TABLE 1. Kinetic Parameters of CdSe Bleaching Recovery

sample	a_1	τ_1 (ps)	a_2	τ_2 (ps)	χ^2	$\langle\tau\rangle$ (ps)	k (10^{10} s^{-1})
1. CdSe	0.03 ± 0.001	14.47 ± 1.27	0.97 ± 0.03	348.3 ± 19.6	0.992	348.0 ± 18.1	0.29 ± 0.01
2. CdSe− MV^{2+}	0.19 ± 0.001	3.26 ± 0.11	0.81 ± 0.03	45.0 ± 2.4	0.997	44.4 ± 2.3	2.25 ± 0.12
3. CdSe−TiO_2	0.07 ± 0.001	16.67 ± 0.87	0.93 ± 0.02	225.9 ± 11.5	0.996	224.7 ± 11.3	0.45 ± 0.23
4. CdSe−TiO_2−MV^{2+}	0.37 ± 0.020	0.62 ± 0.03	0.63 ± 03	4.0 ± 0.2	0.996	3.65 ± 0.11	27.4 ± 0.83

To probe the back electron transfer between $MV^{+\bullet}$ and the holes trapped in CdSe (reaction 5) we performed nanosecond laser flash photolysis experiments. The absorption time profiles recorded following 337 nm laser pulse excitation of CdSe nanoparticles in the absence and presence of MV^{2+} are shown in Figure 5. The formation of $MV^{+\bullet}$ was seen only when the sample was excited in the presence of CdSe. The transient absorption showed a quick decay exhibiting >50% of the signal within 5 μs as $MV^{+\bullet}$ underwent recombination with holes trapped at shallow traps (reaction 5). A significant amount of $MV^{+\bullet}$ eludes this recombination process and remains stable during the probe time scale several 100 μs.

$MV^{+\bullet}$ is stable in inert atmosphere and often serves as a relay to capture and store electrons. When the CdSe−MV^{2+} solution was subjected to steady state illumination we observed an accumulation of $MV^{+\bullet}$ in deaerated AOT/heptane suspension. Figure 6 shows the growth of absorbance at 605 nm corresponding to the accumulation of $MV^{+\bullet}$ with irradiation time (see Supporting Information for the absorption spectra of $MV^{+\bullet}$). A narrow band-pass filter allowed selective excitation of CdSe at 450 ± 10 nm. The photogenerated $MV^{+\bullet}$ attained a steady state concentration of ~36 μM in about 150 s. Although the initial electron transfer (reaction 4) is an ultrafast process, the rate of the back reaction (reaction 5) increases steadily with higher $MV^{+\bullet}$ concentration (or hole concentration), leading to equalization of the rates. Thus, steady state concentration is attained. Upon stopping the illumination we observed a slow decay of the absorption as $MV^{+\bullet}$ undergoes recombination with remaining deep trapped holes and/or oxidized species. The slow back electron transfer occurs with a pseudo-first-order rate constant of $\sim 10^{-2}$ s^{-1}, making the $MV^{2+}/MV^{+\bullet}$ an excellent relay to capture and store electrons. Earlier studies have used this relay and Pt catalyst particles to produce hydrogen.[54,55]

The quantum yield of $MV^{+\bullet}$ was determined using ferrioxalate actinometry.[56] On the basis of the steady state absorbance of $MV^{+\bullet}$ (ε_{605} = 13700 M^{-1} cm^{-1})[62] we obtained a quantum yield of 0.1 for the electron transfer using CdSe as a photocatalyst in a confined medium.

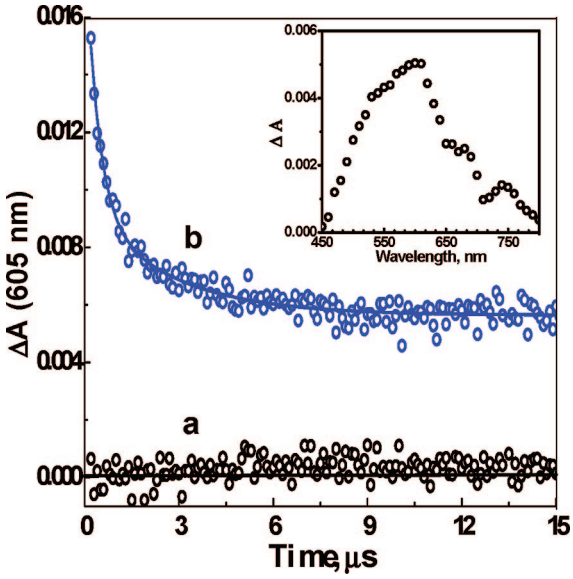

Figure 5. Absorption time profile recorded at 605 nm following 337 nm laser pulse excitation of 2.2 μM CdSe in deaerated AOT/heptane (a) in the absence and (b) presence of 2 mM MV^{2+}. Inset shows trace of the transient absorption spectra of $MV^{+\bullet}$ 10 μs after the pulse.

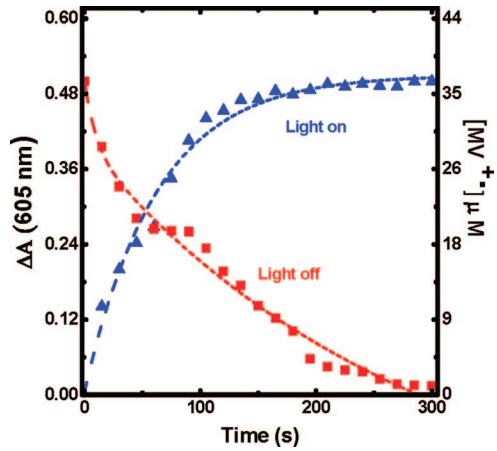

Figure 6. $MV^{+\bullet}$ production following the steady state illumination (450 nm) of 2.2 μM CdSe nanoparticles and 2 mM MV^{2+} and the decay of $MV^{+\bullet}$ upon stopping the illumination.

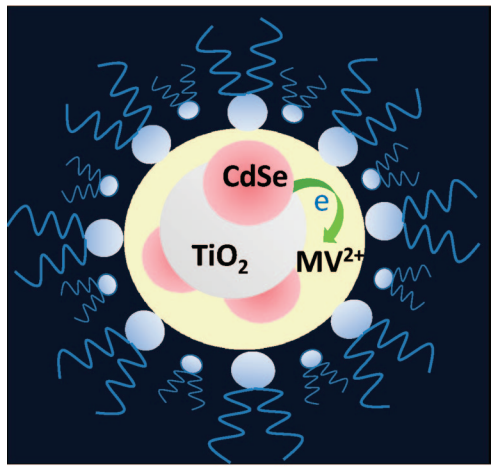

Scheme 2. Coupling CdSe nanoparticles with TiO_2 to boost the efficiency of electron transfer to MV^{2+}.

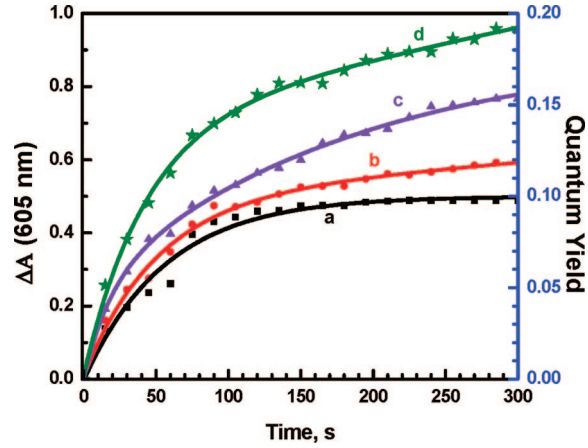

Figure 7. Growth of $MV^{+\bullet}$ concentration with irradiation (450 nm) of CdSe and MV^{2+} solution in AOT/heptane containing different concentrations of TiO_2: (a) 0, (b) 2.5, (c) 10, and (d) 20 μM. The left-hand axis represents absorbance at 605 nm and right-hand axis represents corresponding quantum yields obtained from actinometry.

It should be noted the steady state yield of 10% is significantly lower than the initial transfer of 87% of electrons from excited CdSe into MV^{2+}. The charge recombination processes are responsible for decreased yield in the steady state.

Electron Transfer Mediation with TiO_2 Nanoparticles. One approach to improving the charge separation in a semiconductor particulate system is to couple two semiconductor nanoparticles with suitable energetics (Scheme 2). As shown earlier, charge rectification and charge separation in CdS and CdSe nanoparticles can be greatly improved by coupling them with TiO_2 or ZnO nanoparticles.[12,57,58] In addition, interparticle electron transfer between CdS and TiO_2 in a reverse micellar solution of heptane/water/AOT can be modulated by varying the particle size.[22]

In the present investigation we introduced TiO_2 colloids into a CdSe suspension in AOT/heptane containing MV^{2+} and probed the electron transfer process (Scheme 2). Formation of $MV^{+\bullet}$ in a CdSe−TiO_2 coupled system under steady state irradiation is shown in Figure 7. The beneficial effect of TiO_2 in improving electron transfer yield can be seen from the increase in the $MV^{+\bullet}$ yield with increasing TiO_2 concentration. A 2-fold increase in quantum yield from 0.1 in CdSe to 0.2 in CdSe−TiO_2 systems suggests improved charge separation in the coupled system. It should be noted that the TiO_2 is not subjected to direct excitation since it has no absorption in the visible. The 450 ± 10 nm irradiation thus allows selective excitation of CdSe nanoparticles in a CdSe−TiO_2 composite system.

The improved charge separation and suppression of back electron transfer in CdS/TiO_2 is also indicative of the fact that the Fermi level of the composite becomes more negative (or more reductive) as compared to CdSe alone. By employing a Nernst equation and determining the equilibrium concentration of MV^{2+} and $MV^{+\bullet}$ we estimate Fermi level of −0.343 and −0.361 V *vs* NHE for CdSe and CdSe−TiO_2 systems (see Supporting InformationTable S1 for details). The equilibrated Fermi level of the CdSe−TiO_2 is likely to have synergetic effects in the forward electron transfer as well as higher electron transfer yields.

To assess the role of TiO_2 in enhancing the net electron transfer yield we probed the electron transfer process using femtosecond and nanosecond transient absorption spectroscopy. The bleaching recovery of CdSe absorption band (510 nm) and the absorption of $MV^{+\bullet}$ (605 nm) were monitored to elucidate the effect of TiO_2 on the kinetics and yield of electron transfer (Figures 8 and 9). The recovery of the bleaching was analyzed by biexponential kinetics (equation 6). The lifetimes and average rate constant values are shown in Table 1. Similar to MV^{2+}, TiO_2 also interacts with excited CdSe nanoparticles with electron transfer. The excited-state interaction of CdSe with TiO_2 is reflected in the increased recovery rate of the transient bleaching (reaction 7). In addition we also observe quenching of CdSe emission by TiO_2 (see Supporting InformationFigure S2), providing additional supportive evidence for excited-state interaction between CdSe and TiO_2. The photoinduced reactions between CdSe−TiO_2 and MV^{2+} are summarized in eq 7−9.

$$\text{CdSe (h + e)} + \text{TiO}_2 \rightarrow \text{CdSe (h)} + \text{TiO}_2\text{ (e)} \quad (7)$$

$$\text{TiO}_2\text{ (e)} + \text{MV}^{2+} \rightarrow \text{TiO}_2 + \text{MV}^{+\bullet} \quad (8)$$

$$\text{TiO}_2 + \text{MV}^{+\bullet} \rightarrow \text{TiO}_2\text{ (e)} + \text{MV}^{2+} \quad (9)$$

Because of the close lying energy levels of TiO_2 conduction band and reduction potential of $MV^{2+}/MV^{+\bullet}$ we expect the system to attain quick equilibration *via* reactions 4, 5, 8, and 9. Such a collective interaction of MV^{2+} with CdSe and TiO_2 in AOT/heptane suspension has a pronounced effect on the electron transfer. The

ability of TiO_2 nanoparticles to trap electrons is also likely to influence the overall charge transfer in the composite. Both the recovery of CdSe bleaching and the peak growth at 605 nm show the electron transfer to be extremely fast. The average rate constant of electron transfer observed in the presence of TiO_2 and MV^{2+}, as measured from the CdSe bleaching recovery, was 2.74 $\times$ 10^{11} s^{-1}. This value is significantly higher than the values obtained in the presence of MV^{2+} (k = 2.25 $\times$ 10^{10} s^{-1}) or TiO_2 (k = 4.45 $\times$ 10^9 s^{-1}) alone. It is evident that the presence of both TiO_2 and MV^{2+} in the reverse micelle creates a synergistic effect to provide an order of magnitude enhancement in the electron transfer rate. This rapid rate of electron transfer can also be seen in the growth of $MV^{+\bullet}$ radical. Both the faster rate of electron transfer ($k > 10^{10}$ s^{-1}) and higher absorbance at 605 nm support the assertion that efficient interaction of MV^{2+} and TiO_2 with CdSe yields better charge separation.

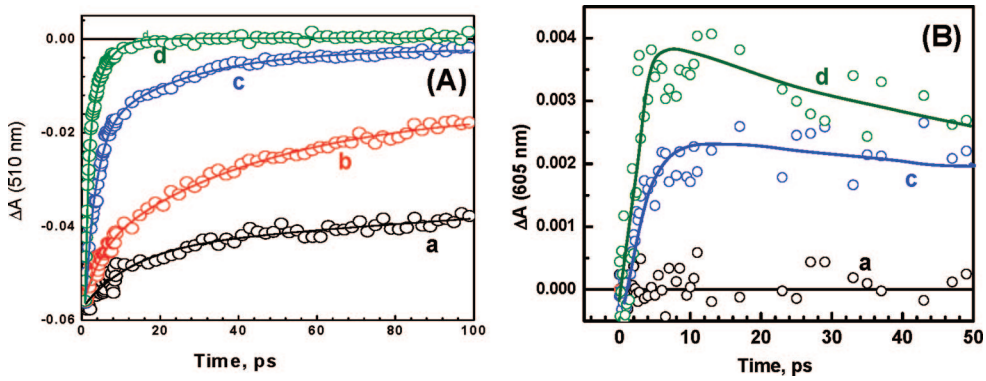

Figure 8. (A) The bleaching recovery at 510 nm and (B) the transient absorption at 605 nm recorded following 387 nm laser pulse excitation of 2.2 μM CdSe nanoparticles in AOT/heptane solution: (a) blank, (b) 20 μM TiO_2; (c) 2 mM MV^{2+}; and (d) 20 μM TiO_2 and 2 mM MV^{2+}.

The role of TiO_2 in improving the long-term survivability of $MV^{+\bullet}$ was probed by nanosecond laser flash photolysis. The transient decay traces were recorded at 605 nm following 337 nm laser pulse excitation of CdSe suspension containing MV^{2+} and different concentrations of TiO_2 (Figure 9). All traces show partial decay during the first few microseconds as the $MV^{+\bullet}$ radicals undergo recombination with holes from shallow traps (reaction 5). The radicals that evade such recombination process stabilize as evident from the unperturbed tail absorption. No detectable transient absorption was seen when CdSe was excluded from the system. Hence, we ruled out contribution arising from direct excitation of TiO_2 or methyl viologen. The recombination rate constant as determined from the first order kinetics of the initial decay in the absence of TiO_2 is 1.1 $\times$ 10^6 s^{-1}. In the presence of TiO_2 the recombination rate slows down, yielding a rate constant of 0.45 $\times$ 10^6 s^{-1}. Thus, the charge recombination rate is reduced by a factor of ~2 when TiO_2 is incorporated into the CdSe−MV^{2+} system. No significant change in the recombination rate constant could be seen at TiO_2 concentrations greater than 10 μM.

The effect of charge stabilization was also evident from the net residual absorption at the end of the decay trace in Figure 9A. We estimated the fraction of the stabilized charge transfer product by determining the ratio of A_{tail}/A_{max}. The residual absorption at the end of the trace was accounted for the absorption due to stabilized charge. The dependence of charge stabilization efficiency ($\eta = A_{tail}/A_{max} \times 100$) on the TiO_2 concentration is shown in Figure 9B. We observed an increase in η (from 28% to 38%) with increasing TiO_2 concentration. The increase in the net charge transfer efficiency highlights the role of TiO_2 in suppressing the back electron transfer process and further supports the observations made in the steady state irradiation experiments. At higher TiO_2 concentrations η reaches a plateau. The nanosecond and femtosecond transient absorption measurements presented here confirm the indirect role of TiO_2 as an electron mediator for promoting the charge transfer between CdSe and MV^{2+} and facilitating charge stabilization with greater efficiency.

The energy levels of CdSe−MV^{2+} and CdSe−TiO_2−MV^{2+} are compared in Scheme 3. The energy levels of these three components dictate the net charge transfer process. While TiO_2 acts as an electron mediator (or electron shuttle), MV^{2+} serves as an elec-

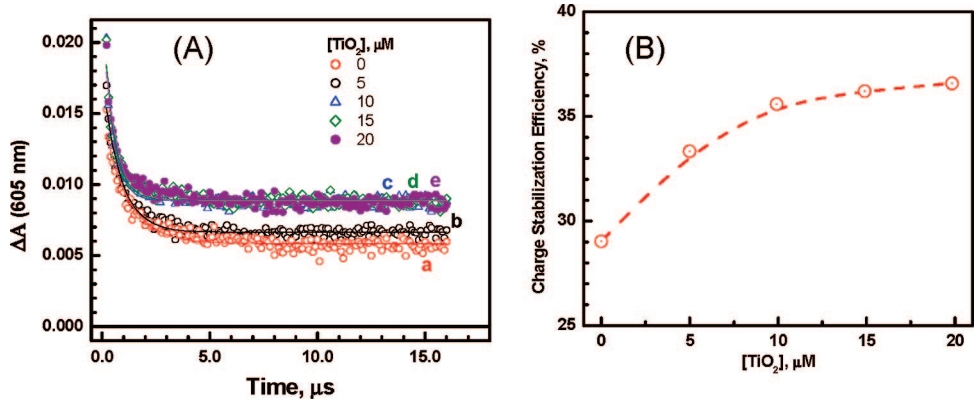

Figure 9. (A) The absorption-time profiles recorded following the laser pulse excitation of 2.2 μM CdSe and 2 mM MV^{2+} in AOT/heptane at different concentration levels of TiO_2; (B) the dependence of charge stabilization efficiency (η) on the TiO_2 concentration.

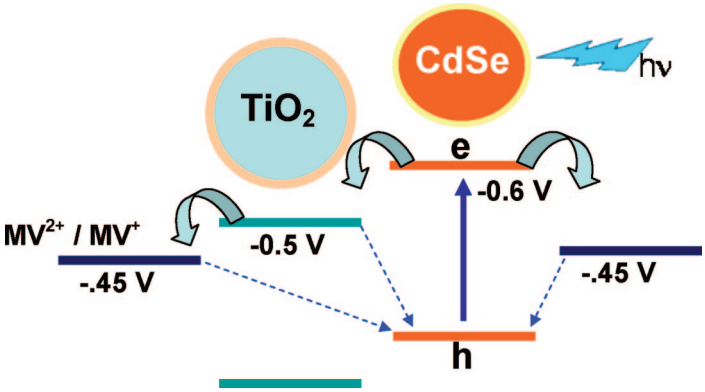

Scheme 3. Energy level diagram (not to scale) illustrating direct and TiO_2-mediated electron transfer from excited CdSe to MV^{2+}. Curved arrows represent forward electron transfer, while dashed arrows represent back electron transfer.

tron sink as the photogenerated electrons are ultimately stored in the form of $MV^{+\bullet}$. To achieve maximum storage ($MV^{+\bullet}$ formation) the electron transfer between these individual components should be fast. In an earlier study Grätzel and co-workers[39,59] reported diffusion controlled electron transfer between TiO_2 and MV^{2+} on a microsecond time scale. Such diffusion limited reduction of MV^{2+} can also arise from other reducing intermediates.[60] In addition, the electrostatic effects induced by surface charge of the semiconductor nanoparticles dictate the rate of electron transfer to MV^{2+}.[61,62]

In the present experiments the electron transfer between excited CdSe and TiO_2 and electron rich TiO_2 and MV^{2+} are ultrafast processes. This observation is in agreement with the ultrafast event of risetime of 10 ps identified previously for the electron transfer between TiO_2 and MV^{2+}.[63] Since all three components ($CdSe-TiO_2-MV^{2+}$) are confined in the polar core of the reverse micelle (Scheme 2), the composite collectively serves as a donor−shuttle−acceptor assembly and thus promotes quick electron transfer to attain charge equilibration. TiO_2 has also been shown to serve as a rectifier in $CdSe-TiO_2$ systems by suppressing the flow of electrons in the reverse direction.[11,64] Thus, TiO_2 in the reverse micelle is able to play dual roles, acting as both an electron shuttle by promoting ultrafast electron transfer to MV^{2+} and as a rectifier by suppressing the charge recombination process between $MV^{+\bullet}$ and trapped holes. The electron transfer in the picosecond time scale as well as the charge stabilization events in the nanoseconds−microseconds−seconds leading to the ultimate accumulation of the electron transfer product highlight intricacies of the charge transfer processes of semiconductor quantum dot systems.

CONCLUSIONS

The transient absorption spectroscopy of CdSe and MV^{2+} in a confined medium (heptane/water/AOT reverse micelle) provides an insight into the electron transfer processes at different time scales. The quenching of excited CdSe by MV^{2+} is an ultrafast charge transfer event that occurs with a rate constant of 2.2×10^{10} s^{-1} ps. The quenching is significantly enhanced in the presence of TiO_2 suggesting a synergistic effect. A net quantum yield of 0.1 was estimated for the production of $MV^{+\bullet}$ in a steady state photoirradiation experiment. The electron transfer yield was enhanced by a factor of 2 by introducing TiO_2 mediator into the system. The role of TiO_2 in suppressing the charge recombination process and stabilization of $MV^{+\bullet}$ radical has been confirmed from the nanosecond laser flash photolysis and steady state photolysis experiments. The electron transfer events as probed by the survivability of $MV^{+\bullet}$ radical at different times (subpicoseconds to seconds) provide an insight into the photocatalytic processes in semiconductor nanoparticle systems. A better understanding of these intermediate charge transfer events is important when designing a photocatalyst for solar hydrogen production or environmental remediation.

EXPERIMENTAL SECTION

Materials. Reagent grade sodium sulfite (anhydrous), perchloric acid (70%), and AOT (sodium salt of dioctyl sulfosuccinate) were purchased from Alfa Aesar. Selenium powder (200 mesh), methyl viologen, anhydrous cadmium sulfate (99% purity), *n*-heptane, and 2-propanol were purchased from Fisher Scientific. Titanium isopropoxide (98% purity) was purchased from Acros.

Absorption and Emission Measurements. Absorption spectra were recorded using a Cary 50 Bio UV−vis spectrophotometer. Emission spectra were recorded with an SLM S-8000C spectrofluorometer. Samples were excited at 400 nm. Emission lifetimes were measured using a Horiba Jobin Yvon single photon counting system. All samples were degassed in N_2.

Laser Flash Photolysis Experiments. The nanosecond laser flash photolysis experiments were conducted using a nitrogen laser, Laser Photonics PRA/model UV-24, operated at 6 mJ/ pulse (337 nm, fwhm-10 ns). Laser excitation was at a right angle with respect to the monitoring light beam. Transient time-absorption profiles were recorded at a preselected wavelength of 605 nm, which corresponds to the characteristic absorption maximum of the methyl viologen radical. The detection system consisted of a pulsed xenon lamp (1kW) as the monitoring light source and SPEX 270 M monochromator coupled with Hamamatsu R955 photomultiplier. The signal from the photomultiplier was processed by a LeCroy 7200 digital storage oscilloscope and a PC-AT compatible computer. Rectangular quartz cells with dimensions 0.5×1 cm were used. Typically 10−15 laser shots were averaged to record each kinetic trace. All solutions were deaerated by purging with N_2.

Femtosecond Transient Absorption Spectroscopy. Ultrafast transient absorption experiments were conducted using a Clark-MXR 2010 laser system (387 nm, 1 mJ/pulse, fwhm 130 fs, 1 kHz repetition rate) and an Ultrafast Systems (Helios) detection system. The white light probe was generated by feeding 5% of the fundamental laser output (775 nm) through an optical delay line and focusing it on a quartz crystal. The optical delay provided a probe time window of 1.6 ns with a step resolution of 7 fs. The

pump beam was attenuated at 5 μJ/pulse with a spot size of 2 mm (diameter) at the sample position where it was merged with the white light incident on the sample cell at an angle <10°. After passing through the sample the probe beam was focused on a 200 μm core fiber connected to an Ocean Optics S2000 UV−vis CCD spectrograph (425−800 nm). Typically 1000 excitation pulses were averaged to obtain the transient spectrum at a set delay time. Kinetic traces at appropriate wavelengths were assembled from the time-resolved data. All measurements were conducted at room temperature by flowing deaerated sample through a quartz flow cell.

Steady State Absorption Spectra. The Ocean Optics S-2000 UV−vis CCD Spectrograph was used to record absorption spectra in real time at preset time intervals. The deaerated sample was concurrently excited with a collimated light from 250 W xenon lamp passed through a 450 nm bandpass filter. CCD integration time was 300 ms and each data point was an average of 15 measurements.

Preparation of CdSe Colloids. A stock solution of 0.10 M sodium selenosulfate, Na_2SeSO_3, was prepared by adding 0.395 g of Se powder and 1.26 g of Na_2SO_3 to 50 mL of distilled water.[24] The solution was held at 70 °C for 24 h and a clear solution was obtained. Two separate micelle solutions of equal w_o were prepared. In one vial 150 μL of 1 M $CdSO_4$ and 850 μL of distilled water were added to 15 mL of 0.394 M AOT in heptane. In the second vial 900 μL of 0.1 M Na_2SeSO_3 and 100 μL of distilled water were added to an equal volume (15 mL) of 0.394 M AOT/heptane. The two solutions were then mixed under vigorous stirring to produce CdSe particles. The net reaction is shown in reaction 10. The suspension was stirred for an additional 2 h so that the growth process was completed. An excess of Cd^{2+} was used to ensure the neutralization of $SeSO_3^{2-}$ and thus control the overall growth of particles.

$$Cd^{2+} + SeSO_3^{2-} + 2OH^- \rightarrow CdSe + SO_4^{2-} + H_2O \qquad (10)$$

Preparation of the TiO_2 Colloids. TiO_2 nanoparticles in reverse micellar suspension were synthesized *via* hydrolysis of a Ti−alkoxide precursor. Dropwise addition of a titanium isopropoxide/2-propanol solution to a micellar solution (0.394 M AOT/heptane) containing dilute $HClO_4$ (aq) under mild mixing produced a stable suspension of TiO_2 nanoparticles. The presence of dilute $HClO_4$ (~0.001 M) facilitates stabilization of the TiO_2 nanoparticles and prevents particle growth during storage.[22]

Acknowledgement The research described herein was supported by the Department of Energy, Office of Basic Sciences. We would like to thank Dr. Dan Meisel for helpful discussions and Dr. Gordon Hug for his assistance in the nanosecond laser flash photolysis experiments. This is contribution number NDRL 4790 from the Notre Dame Radiation Laboratory.

Supporting Information Available: Results illustrating emission quenching by TiO_2, quenching analysis, absorption spectrum of $MV^{+\bullet}$, TEM image of CdSe particles, and association constant calculations are presented in the Supporting Information. This material is available free of charge *via* the Internet at http://pubs.acs.org.

REFERENCES AND NOTES

1. Kamat, P. V. Meeting the Clean Energy Demand: Nanostructure Architectures for Solar Energy Conversion. *J. Phys. Chem. C* **2007**, *111*, 2834–2860.
2. Kamat, P. V. Quantum Dot Solar Cells. Semiconductor Nanocrystals as Light Harvesters. *J. Phys. Chem. C* **2008**, *112*, 18737–18753.
3. Kamat, P. V. Photochemistry on Nonreactive and Reactive (Semiconductor) Surfaces. *Chem. Rev.* **1993**, *93*, 267–300.
4. Thompson, T. L.; Yates, J. T. TiO_2-Based Photocatalysis: Surface Defects, Oxygen and Charge Transfer. *Top. Catal.* **2005**, *35*, 197–210.
5. Tachikawa, T.; Fujitsuka, M.; Majima, T. Mechanistic Insight into the TiO_2 Photocatalytic Reactions: Design of New Photocatalysts. *J. Phys. Chem. C* **2007**, *111*, 5259–5275.
6. Nowotny, M. K.; Sheppard, L. R.; Bak, T.; Nowotny, J. Defect Chemistry of Titanium Dioxide. Application of Defect Engineering in Processing of TiO_2-Based Photocatalysts. *J. Phys. Chem. C* **2008**, *112*, 5275–5300.
7. Kamat, P. V.; Meisel, D. Nanoparticles in Advanced Oxidation Processes. *Curr. Opin. Colloid Interface Sci.* **2002**, *7*, 282–287.
8. Peller, J.; Wiest, O.; Kamat, P. V. Hydroxyl Radical's Role in the Remediation of a Common Herbicide, 2,4-Dichlorophenoxyacetic Acid (2,4-D) - Feature Article. *J. Phys. Chem. A* **2004**, *108*, 10925–10933.
9. Gerischer, H.; Luebke, M. A Particle Size Effect in the Sensitization of TiO_2 Electrodes by a CdS Deposit. *J. Electroanal. Chem.* **1986**, *204*, 225–227.
10. Spanhel, L.; Weller, H.; Henglein, A. Photochemistry of Semiconductor Colloids. 22. Electron Injection from Illuminated CdS into Attached TiO_2 and ZnO Particles. *J. Am. Chem. Soc.* **1987**, *109*, 6632–6635.
11. Liu, D.; Kamat, P. V. Photoelectrochemical Behavior of Thin CdSe and Coupled TiO_2/CdSe Semiconductor Films. *J. Phys. Chem.* **1993**, *97*, 10769–10773.
12. Gopidas, K. R.; Bohorquez, M.; Kamat, P. V. Photoelectrochemistry in Semiconductor Particulate Systems. 16. Photophysical and Photochemical Aspects of Coupled Semiconductors. Charge-transfer Processes in Colloidal CdS-TiO_2 and CdS-AgI Systems. *J. Phys. Chem.* **1990**, *94*, 6435–6440.
13. Hotchandani, S.; Kamat, P. V. Charge-transfer Processes in Coupled Semiconductor Systems. Photochemistry and Photoelectrochemistry of the Colloidal CdS-ZnO System. *J. Phys. Chem.* **1992**, *96*, 6834–6839.
14. Leschkies, K. S.; Divakar, R.; Basu, J.; Enache-Pommer, E.; Boercker, J. E.; Carter, C. B.; Kortshagen, U. R.; Norris, D. J.; Aydil, E. S. Photosensitization of ZnO Nanowires with CdSe Quantum Dots for Photovoltaic Devices. *Nano Lett.* **2007**, *7*, 1793–1798.
15. Tena-Zaera, R.; Katty, A.; Bastide, S.; Levy-Clement, C. Annealing Effects on the Physical Properties of Electrodeposited ZnO/CdSe Core−Shell Nanowire Arrays. *Chem. Mater.* **2007**, *19*, 1626–1632.
16. Nasr, C.; Hotchandani, S.; Kamat, P. V. CdSe/SnO_2 Coupled Semiconductor Films. Electrochemical and Photoelectrochemical Studies. *Proc. Ind. Acad. Sci.* **1995**, *107*, 699–708.
17. Shen, Q.; Yanai, M.; Katayama, K.; Sawada, T.; Toyoda, T. Optical Absorption, Photosensitization, and Ultrafast Carrier Dynamic Investigations of CdSe Quantum Dots Grafted onto Nanostructured SnO_2 Electrode and Fluorine-doped Tin Oxide (FTO) Glass. *Chem. Phys. Lett.* **2007**, *442*, 89–96.
18. Serpone, N. Relative Phtotonic Efficiencies and Quantum Yields in Heterogeneous Photocatalysis. *J. Photochem. Photobiol., A: Chem.* **1997**, *104*, 1–12.
19. Pileni, M. P. Reverse Micelles as Microreactors. *J. Phys. Chem.* **1993**, *97*, 6961–6973.
20. Petit, C.; Pileni, M. P. Synthesis of Cadmium Sulfide *in Situ* in Reverse Micelles and in Hydrocarbon Gels. *J. Phys. Chem.* **1988**, *92*, 2282–6.
21. Lianos, P.; Thomas, J. K. Small CdS Particles in Inverted Micelles. *J. Colloid Interface Sci.* **1986**, *117*, 505–512.
22. Sant, P. A.; Kamat, P. V. Inter-particle Electron Transfer between Size-Quantized CdS and TiO_2 Semiconductor Nanoclusters. *Phys. Chem. Chem. Phys.* **2002**, *4*, 198–203.
23. Fujii, H.; Inata, K.; Ohtaki, M.; Eguchi, K.; Arai, H. Synthesis of TiO_2/CdS Nanocomposite *via* TiO_2 Coating on CdS Nanoparticles by Compartmentalized Hydrolysis of Ti Alkoxide. *J. Mater. Sci.* **2001**, *36*, 527–532.
24. Chandrasekharan, N.; Kamat, P. V. Tuning the Properties of CdSe Nanoparticles in Reverse Micelles. *Res. Chem. Intermed.* **2002**, *28*, 847–856.

25. Nave, S.; Paul, A.; Eastoe, J.; Pitt, A. R.; Heenan, R. K. What is so Special about Aerosol-OT? Part IV. Phenyl-Tipped Surfactants. *Langmuir* **2005**, *21*, 10021–10027.
26. Zulauf, M.; Eicke, H.-F. Inverted Micelles and Microemulsions in the Ternary System H_2O/Aerosol-OT/Isooctane as Studied by Photon Correlation Spectroscopy. *J. Phys. Chem.* **1979**, *83*, 480–486.
27. Murray, C.; Norris, D.; Bawendi, M. Synthesis and Characterization of Nearly Monodisperse CdE (E = S, Se, Te) Semiconductor. *J. Am. Chem. Soc.* **1993**, *115*, 8706–8715.
28. Raevskaya, A. E.; Stroyuk, A. L.; Kuchmiy, S. Y. Preparation of Colloidal CdSe and CdS/CdSe Nanoparticles from Sodium Selenosulfate in Aqueous Polymers Solutions. *J. Colloid Interface Sci.* **2006**, *302*, 133–141.
29. Dimitrijevic, N. M. Electron-Transfer Reactions on CdSe Colloids as Studied by Pulse Radiolysis. *J. Chem. Soc., Faraday Trans. 1* **1987**, *83*, 1193–201.
30. Burda, C.; Green, T. C.; Link, S.; El-Sayed, M. A. Electron Shuttling Across the Interface of CdSe Nanoparticles Monitored by Femtosecond Laser Spectroscopy. *J. Phys. Chem. B* **1999**, *103*, 1783–1788.
31. Sharma, S.; Pillai, Z. S.; Kamat, P. V. Photoinduced Charge Transfer between CdSe Nanocrystals and *p*-Phenylenediamine. *J. Phys. Chem. B* **2003**, *107*, 10088–10093.
32. Robel, I.; Subramanian, V.; Kuno, M.; Kamat, P. V. Quantum Dot Solar Cells. Harvesting Light Energy with CdSe Nanocrystals Molecularly Linked to Mesoscopic TiO_2 Films. *J. Am. Chem. Soc.* **2006**, *128*, 2385–2393.
33. Robel, I.; Kuno, M.; Kamat, P. V. Size-Dependent Electron Injection from Excited CdSe Quantum Dots into TiO_2 Nanoparticles. *J. Am. Chem. Soc.* **2007**, *129*, 4136–4137.
34. Ginger, D. S.; Greenham, N. C. Photoinduced Electron Transfer from Conjugated Polymers to CdSe Nanocrystals. *Phys. Rev. B* **1999**, *59*, 10622–10629.
35. Huang, J.; Stockwell, D.; Huang, Z. Q.; Mohler, D. L.; Lian, T. Q. Photoinduced Ultrafast Electron Transfer from CdSe Quantum Dots to Re-bipyridyl complexes. *J. Am. Chem. Soc.* **2008**, *130*, 5632–5633.
36. Scholes, G. D. Insights into Excitons Confined to Nanoscale Systems: Electron−Hole Interaction, Binding Energy, and Photodissociation. *ACS Nano* **2008**, *2*, 523–537.
37. Jones, M.; Kumar, S.; Lo, S. S.; Scholes, G. D. Exciton Trapping and Recombination in Type II CdSe/CdTe Nanorod Heterostructures. *J. Phys. Chem. C* **2008**, *112*, 5423–5431.
38. Wang, C. J.; Shim, M.; Guyot-Sionnest, P. Electrochromic Nanocrystal Quantum Dots. *Science* **2001**, *291*, 2390–2392.
39. Graetzel, M.; Frank, A. J. Interfacial Electron-transfer Reactions in Colloidal Semiconductor Dispersions. Kinetic Analysis. *J. Phys. Chem.* **1982**, *86*, 2964−2967.
40. Dimitrijevic, N. M.; Kamat, P. V. Transient Photobleaching of Small CdSe Colloids in Acetonitrile. Anodic Decomposition. *J. Phys. Chem.* **1987**, *91*, 2096–2099.
41. Zhang, J. Z. Interfacial Charge Carrier Dynamics of Colloidal Semiconductor Nanoparticles. *J. Phys. Chem. B* **2000**, *104*, 7239–7253.
42. Shen, Q.; Katayama, K.; Yamaguchi, M.; Sawada, T.; Toyoda, T. Study of Ultrafast Carrier Dynamics of Nanostructured TiO_2 Films with and without CdSe Quantum Dot Deposition Using Lens-free Heterodyne Detection Transient Grating Technique. *Thin Solid Films* **2005**, *486*, 15–19.
43. Lee, H. J.; Yum, J.-H.; Leventis, H. C.; Zakeeruddin, S. M.; Haque, S. A.; Chen, P.; Seok, S. I.; Gratzel, M.; Nazeeruddin, M. K. CdSe Quantum Dot-Sensitized Solar Cells Exceeding Efficiency 1% at Full-Sun Intensity. *J. Phys. Chem. C* **2008**, *112*, 11600–11608.
44. Borgarello, E.; Pelizzetti, E.; Mulac, W. A.; Meisel, D. Electron-Transfer and Dimerization of Viologen Radicals on Colloidal TiO_2. *J. Am. Chem. Soc., Faraday Trans. 1* **1985**, *81*, 143–159.
45. Yu, W. W.; Qu, L. H.; Guo, W. Z.; Peng, X. G. Experimental Determination of the Extinction Coefficient of CdTe, CdSe, and CdS Nanocrystals. *Chem. Mater.* **2003**, *15*, 2854–2860.
46. Kamat, P. V.; Chauvet, J. P.; Fessenden, R. W. Photoelectrochemistry in Particulate Systems. 4. Photosensitization of a TiO_2 Semiconductor with a Chlorophyll Analogue. *J. Phys. Chem.* **1986**, *90*, 1389−94.
47. Logunov, S.; Green, T.; Marguet, S.; El-Sayed, M. A. Interfacial Carriers Dynamics of CdS Nanoparticles. *J. Phys. Chem. A* **1998**, *102*, 5652–5658.
48. Underwood, D. F.; Kippeny, T.; Rosenthal, S. J. Charge Carrier Dynamics in CdSe Nanocrystals: Implications for the Use of Quantum Dots in Novel Photovoltaics. *Eur. Phys. J. D* **2001**, *16*, 241–244.
49. Klimov, V.; Bolivar, P. H.; Kurz, H. Ultrafast Carrier Dynamics in Semiconductor Quantum Dots. *Phys. Rev. B* **1996**, *53*, 1463–1467.
50. Klimov, V. I.; McBranch, D. W. Femtosecond 1P-to-1S Electron Relaxation in Strongly Confined Semiconductor Nanocrystals. *Phys. Rev. Lett.* **1998**, *80*, 4028–4031.
51. Burda, C.; Link, S.; Mohamed, M.; El-Sayed, M. The Relaxation Pathways of CdSe Nanoparticles Monitored with Femtosecond Time-Resolution from the Visible to the IR: Assignment of the Transient Features by Carrier Quenching. *J. Phys. Chem. B* **2001**, *105*, 12286–12292.
52. Peng, P.; Milliron, D. J.; Hughes, S. M.; Johnson, J. C.; Alivisatos, A. P.; Saykally, R. J. Femtosecond Spectroscom of Carrier Relaxation Dynamics in Type II CdSe/CdTe Tetrapod Heteronanostructures. *Nano Lett.* **2005**, *5*, 1809–1813.
53. James, D. R.; Liu, Y.-S.; de Mayo, P.; Ware, W. R. Distributions of Fluorescence Lifetimes: Consequences for the Photophysics of Molecules Adsorbed on Surfaces. *Chem. Phys. Lett.* **1985**, *120*, 460.
54. Miller, D. S.; Bard, A. J.; McLendon, G.; Ferguson, J. Catalytic Water Reduction at Colloidal Metal "Microelectrodes". 2. Theory and Experiment. *J. Am. Chem. Soc.* **1981**, *103*, 5336–5341.
55. Borgarello, E.; Kiwi, J.; Pelizzetti, E.; Visca, M.; Graetzel, M. Photochemical Cleavage of Water by Photocatalysis. *Nature* **1981**, *289*, 158–160.
56. Murov, S. L.; Hug, G. L.; Carmichael, I. *Handbook of Photochemistry*, 2nd ed.; M. Dekker: New York, 1993; *Vol. viii*, p 420.
57. Willner, I.; Eichen, Y. TiO_2 and CdS Colloids Stabilized by beta-Cyclodextrins: Tailored Semiconductor−Receptor Systems as a Means to Control Interfacial Electron-Transfer Processes. *J. Am. Chem. Soc.* **1987**, *109*, 6862–6863.
58. Lawless, D.; Kapoor, S.; Meisel, D. Bifunctional Capping of CdS Nano-particles and Bridging to TiO_2. *J. Phys. Chem.* **1995**, *99*, 10329–10335.
59. Duonghong, D.; Ramsden, J.; Graetzel, M. Dynamics of Interfacial Electron-Transfer Processes in Colloidal Semiconductor Systems. *J. Am. Chem. Soc.* **1982**, *104*, 2977–2985.
60. Bahnemann, D.; Henglein, A.; Lilie, J.; Spanhel, L. Flash Photolysis Observation of the Absorption Spectra of Trapped Positive Holes and Electrons in Colloidal TiO_2. *J. Phys. Chem.* **1984**, *88*, 709–711.
61. Brown, G. T.; Darwent, J. R.; Fletcher, P. D. I. Interfacial Electron Transfer in TiO_2 Colloids. *J. Am. Chem. Soc.* **1985**, *107*, 6446–6451.
62. Mulvaney, P.; Swayambunathan, V.; Grieser, F.; Meisel, D. Dynamics of Interfacial Charge Transfer in Iron(III) Oxide Colloids. *Phys. Chem.* **1988**, *92*, 6732–6740.
63. Asahi, T.; Furube, A.; Masuhara, H. Direct Measurement of Picosecond Interfacial Electron Transfer from Photoexcited TiO_2 Powder to an Adsorbed Molecule in the Opaque Suspension. *Chem. Phys. Lett.* **1997**, *275*, 234–238.
64. Liu, D.; Kamat, P. V. Electrochemical Rectification in CdSe + TiO_2 Coupled Semiconductor Films. *J. Electroanal. Chem. Interfacial Electrochem.* **1993**, *347*, 451–456.